

# 1 **Large nuisance modulation has little impact on IT target match** 2 **performance**

3  
4 Noam Roth, Nicole C. Rust<sup>1</sup>  
5 Department of Psychology, University of Pennsylvania, Philadelphia, PA

6  
7 <sup>1</sup>Corresponding author.

## 8 9 **Summary:**

10  
11 Many everyday tasks require us to extract a specific type of information from our environment  
12 while ignoring other things. When the neurons in our brains that carry task-relevant signals are  
13 also modulated by task-irrelevant “nuisance” information, nuisance modulation is expected to  
14 act as performance-limiting noise. To investigate the impact of nuisance modulation on neural  
15 task performance, we recorded responses in inferotemporal cortex (IT) as monkeys performed a  
16 task in which they were rewarded for indicating when a target object appeared amid  
17 considerable nuisance variation. Within IT, we found a robust, behaviorally-relevant target  
18 match signal that was mixed with large nuisance modulations in individual neurons.  
19 Unexpectedly, we also found that these nuisance modulations had little impact on performance,  
20 either within individual IT neurons or across the IT population. We demonstrate how these  
21 results follow from fast processing in IT, which placed IT in a low spike count regime where the  
22 impact of nuisance variability was blunted by Poisson-like trial variability. These results  
23 demonstrate that some basic intuitions about neural coding are misguided in the context of a  
24 fast-processing, low spike count regime.

## 25 26 **Introduction:**

27  
28 Task performance is determined not only by the amount of task-relevant signal present in our  
29 brains, but also by the presence of noise, which can arise from multiple sources. Internal noise,  
30 or “trial variability” manifests as trial-by-trial variations in neural responses under seemingly  
31 identical conditions (Fig 1a). External factors can also translate into noise, particularly when a  
32 task requires extracting a particular type of information from our environment amid changes in  
33 other task-irrelevant, nuisance parameters (Fig 1b; Haefner and Bethge, 2010; Kim et al., 2016).  
34 Stated differently, for any given task, neurons in a brain area may be modulated by multiple  
35 experimental variables, but when viewed from the perspective of task performance, one type of  
36 modulation reflects the task-relevant signal, whereas other types of modulations act as noise.

37  
38 Despite notions that mixing different types of signals within the responses of individual neurons  
39 should be detrimental for task performance (Fig 1b), growing evidence suggests that the brain  
40 does often mix them, both at the locus at which task-relevant solutions are computed as well as  
41 downstream (Freedman and Assad, 2009; Kobak et al., 2016; Mante et al., 2013; Meister et al.,  
42 2013; Raposo et al., 2014; Rigotti et al., 2013; Rishel et al., 2013; Zoccolan et al., 2007). One  
43 example is visual target search, which requires the brain to compare incoming visual information  
44 with a remembered representation of a target to create a signal that reports when a target match  
45 is in view. When considered across changes in target identity (e.g. looking for your car keys  
46 and then your wallet), target search can be envisioned as differentiating the same images  
47 presented as target matches versus as distractors (e.g. when looking for your car keys, your

48 wallet is a distractor; when looking for your wallet, your car keys are distractor and your wallet is  
49 a target match). Consequently, other types of modulation, such as visual modulation (e.g.  
50 signals that differentiate wallets and car keys regardless of what you are searching for), act as  
51 noise. A number of lines of evidence suggest that target match information emerges in the  
52 ventral visual pathway as early as V4 (Kosai et al., 2014; Maunsell et al., 1991) and  
53 inferotemporal cortex (IT, Chelazzi et al., 1993; Eskandar et al., 1992; Leuschow et al., 1994;  
54 Miller and Desimone, 1994; Pagan et al., 2013), where nuisance modulation, including visual  
55 modulation, is expected to be large. This suggests that nuisance modulation may place strong  
56 limitations on neural target match performance in these ventral visual pathway brain areas.

57  
58 Understanding how nuisance modulation affects neural task performance requires considering  
59 its impact in individual neurons as well as across the population. Investigations, focused in part  
60 on view-invariant object recognition, have demonstrated the means by which individual neurons  
61 can multiplex different types of signals such that each type of signal can be extracted from the  
62 population with a simple linear decoder (DiCarlo and Cox, 2007; Hong et al., 2016; Hung et al.,  
63 2005; Li et al., 2009). But little attention has been directed toward understanding how signal  
64 mixing impacts population performance within the context of these linearly separable  
65 representations – e.g. under what conditions would a linearly separable population be better off  
66 to parse different signals into non-overlapping subpopulations versus mix them? Some insight  
67 into these issues can be gained from work focused on how correlated interactions between  
68 neurons impacts population performance within a linear decoding scheme (reviewed by  
69 Averbeck et al., 2006; Cohen and Kohn, 2011; Kohn et al., 2016). However, this work has  
70 focused nearly exclusively on correlated trial (as opposed to nuisance) variability (but see Kim et  
71 al., 2016). Understanding how nuisance modulation impacts neural task performance will thus  
72 require extending these population-based approaches to incorporate considerations about  
73 nuisance modulation.

74  
75 To investigate the impact of nuisance modulation on IT target match performance, we recorded  
76 neural signals in IT as monkeys performed a modified delayed-match-to-sample task in which  
77 they were rewarded for indicating when a target object appeared across changes in the objects'  
78 position, size and background context (Fig 2). Our study was motivated by the simple intuition  
79 that when neurons are modulated not only by task-relevant signals but also by large, task-  
80 irrelevant nuisance modulations, nuisance modulations should act as a source of noise that  
81 limits task performance (Fig 1b). As described in more detail below, we did indeed find a robust,  
82 behaviorally-relevant target match signal in IT that was in fact mixed with even larger nuisance  
83 modulations within the responses of individual IT units. Unexpectedly, we also found that these  
84 large nuisance modulations had little impact on neural task performance. We reconciled these  
85 seemingly discrepant results by also considering another source of noise, trial variability, which  
86 was considerably larger than both signal and nuisance modulations. As we demonstrate below,  
87 large trial variability acts to blunt the impact of nuisance modulation on task performance, both  
88 within individual IT units and across the IT population.

89  
90

## 91 **Results:**

92

### 93 ***The invariant delayed-match-to-sample task (IDMS)***

94

95 To investigate the degree to which nuisance modulation impacts neural task performance, we  
96 trained two monkeys to perform an “invariant delayed-match-to-sample” (IDMS) task that  
97 required them to report when target objects appeared across variation in the objects’ positions,  
98 sizes and background contexts. In this task, the target object was held fixed for short blocks of  
99 trials (~3 minutes on average) and each block began with a cue trial indicating the target for that  
100 block (Fig 2a, “Cue trial”). Subsequent test trials always began with the presentation of a  
101 distractor and on most trials this was followed by 0-5 additional distractors (for a total of 1-6  
102 distractor images) and then an image containing the target match (Fig 2a, “Test trial”). The  
103 monkeys’ task required them to fixate during the presentation of distractors and make a saccade  
104 to a response dot on the screen following target match onset to receive a reward. To minimize  
105 the predictability of the match appearing as a trial progressed, on a small subset of the trials the  
106 match did not appear and the monkey was rewarded for maintaining fixation. Our experimental  
107 design differs from other classic DMS tasks (Chelazzi et al., 1993; Eskandar et al., 1992;  
108 Leuschow et al., 1994; Miller and Desimone, 1994; Pagan et al., 2013) in that it does not  
109 incorporate a cue at the beginning of each test trial, to better mimic real-world object search  
110 conditions in which target matches are not repeats of the same image presented shortly before.

111

112 Our experiment included a fixed set of 20 images, broken down into 4 objects presented at each  
113 of 5 transformations (Fig 2b). Our goal in selecting these specific images was to make the task  
114 of classifying object identity challenging for the IT population and these specific transformations  
115 were built on findings from our previous work (Rust and DiCarlo, 2010). In any given block (e.g.  
116 a squirrel target block), a subset of 5 of the images would be considered target matches and the  
117 remaining 15 would be distractors (Fig 2b). Our full experimental design amounted to 20 images  
118 (4 objects presented at 5 identity-preserving transformations), all viewed in the context of each  
119 of the 4 objects as a target, resulting in 80 experimental conditions (Fig 2c). In this design,  
120 “target matches” fall along the diagonals of each looking at / looking for matrix slice (where  
121 “slice” refers to a fixed transformation; Fig 2c, gray). For each condition, we collected at least 20  
122 repeats on correct trials. Monkeys generally performed well on this task (Fig 2d). Their mean  
123 reaction times (computed as the time their eyes left the fixation window relative to the target  
124 match stimulus onset) were 366 ms and 332 ms (Fig 2e).

125

126 As two monkeys performed this task, we recorded neural activity from small populations in  
127 inferotemporal cortex (IT) using 24-channel probes. We performed two types of analyses on  
128 these data. The first type of analysis was performed on the data recorded simultaneously across  
129 units within a single recording session (n=21 sessions). The second type of analysis was  
130 performed on data that was concatenated across different sessions to create a  
131 pseudopopulation after screening for units based on their stability, isolation, and task modulation  
132 (see Methods; n=235 units). For all but one of our analyses (Fig 4d), we counted spikes in a  
133 window that started 80 ms following stimulus onset (to allow stimulus-evoked responses time to  
134 reach IT) and ended at 250 ms, which was always before the monkeys’ reaction times on these  
135 trials. For all but one of our analyses (Fig 3c), the data are extracted from trials with correct  
136 responses.

137

138

139 **IT reflects behaviorally-relevant target match information**

140

141 The primary focus of this report is the impact of mixing signal and nuisance modulation on  
142 neural task performance. Before exploring the consequences of nuisance modulation, we begin  
143 by demonstrating that behaviorally-relevant target match information is in fact reflected in IT  
144 during the IDMS task.

145

146 The IDMS task required monkeys to determine whether each condition (an image viewed in the  
147 context of a particular target) was a target match or a distractor. This task ultimately maps all  
148 the target match conditions onto one behavioral response (a saccade) and all the distractor  
149 conditions onto another (maintain fixation), and as such, this task can be envisioned as a two-  
150 way classification that must be performed invariant to changes in other nuisance parameters,  
151 including changes in target and image identity (Fig 3a). To quantify the amount and format of  
152 target match information within IT, we began by quantifying cross-validated performance of this  
153 two-way classification with a linear population decoder (a Fisher Linear Discriminant, FLD).  
154 Linear decoder performance began near chance and grew as a function of population size,  
155 consistent with a robust IT target match representation (Fig 3b, black). To determine the degree  
156 to which a component of IT target match information might be present in a nonlinear format that  
157 could not be accessed by a linear decoder, we measured the performance of a maximum  
158 likelihood decoder designed to extract target match information regardless of its format  
159 (combined linear and nonlinear, Pagan et al., 2013, see Methods). Performance of this  
160 nonlinear decoder (Fig 3b, gray) was slightly higher and significantly better than linear decoder  
161 performance, suggesting that while the majority of IT target match information is reflected in a  
162 linearly separable format, a smaller nonlinear component exists as well.

163

164 Upon establishing the format of target match information on correct trials, we were interested in  
165 determining the degree to which behavioral confusions were reflected in the IT neural data. To  
166 measure this, we focused on the data recorded simultaneously across multiple units within each  
167 session, where all units observed the same errors. With this data, we trained the linear decoder  
168 to perform the same target match versus distractor classification described for Fig 3b using data  
169 from correct trials, and we measured cross-validated performance on pairs of condition-matched  
170 trials: one for which the monkey answered correctly, and the other for which the monkey made  
171 an error. On correct trials, target match decoder performance grew with population size and  
172 reached levels significantly above chance in populations of 24 units (Fig 3c, black). On error  
173 trials, decoder performance fell significantly below chance, and these results replicated across  
174 each monkey individually (Fig 3c, white). These results establish that IT reflects behaviorally-  
175 relevant target match information insofar as this measure co-varies with the monkeys' behavior.

176

177 We were also interested in understanding how target match modulation was reflected in  
178 individual units. Target match modulation, by definition, requires a differential response to the  
179 same images presented as matches versus as distractors - to what degree is this modulation  
180 reflected by firing rate increases versus decreases? To measure this, we computed a target  
181 match modulation index for each unit as the average difference between the responses to the  
182 same images presented as target matches versus as distractors, divided by the sum of those  
183 two quantities. This index (Fig 3d) was shifted toward target match preferring units, with a mean  
184 value of 1.0 (monkey 1 = 1.21; monkey 2 = 0.70). These results are consistent with a target  
185 match signal that is largely reflected in most IT neurons via increased responses to target  
186 matches as compared to distractors.

187

188

189 ***During the IDMS task, nuisance modulation is prominent***

190

191 As described above, we were interested in understanding whether and how nuisance  
192 modulation impacted IT target match performance. As a first step toward addressing this  
193 question, we wanted to quantify the relative amounts of target match and nuisance modulation  
194 present within individual units. To quantify the different types of modulation reflected in IT, we  
195 applied a bias-corrected procedure that quantified different types of modulation in terms of the  
196 number of standard deviations around each unit's grand mean spike count (Pagan and Rust,  
197 2014b). Modulation types were grouped into intuitive sets, including modulation that could be  
198 attributed to whether each condition was a target match or a distractor (the "target match"  
199 signal), modulation due to changes in the identity of the visual stimulus ("visual"), modulation  
200 due to changes in the identity of the target ("target"), and "residual" modulations attributed to  
201 nonlinear interactions between the visual stimulus and target that were not captured by target  
202 match modulation (e.g. specific distractor conditions). We also combined all the different types  
203 of "nuisance" modulation into one measure for each neuron.

204

205 Our measure of modulation is similar to a multi-way ANOVA, with important extensions.  
206 Specifically, a two-way ANOVA applied to a unit's responses (configured into a matrix of 4  
207 targets \* 20 images \* 20 trials for each condition) would parse the total response variance into  
208 two linear terms, a nonlinear interaction term, and an error term. We make 3 extensions to the  
209 ANOVA analysis. First, an ANOVA returns measures of variance (in units of spike counts  
210 squared) whereas we compute measures of standard deviation (in units of spike count) such  
211 that our measures of modulation are intuitive (e.g., doubling firing rates causes signals to double  
212 as opposed to quadruple). Second, while the linear terms of the ANOVA map onto our "visual"  
213 and "target" modulations (after squaring), we split the ANOVA nonlinear interaction term into two  
214 terms, including target match modulation (i.e. Fig 2c gray versus white) and all other nonlinear  
215 "residual" modulation. This parsing is essential, as target match modulation corresponds to the  
216 signal for the IDMS task whereas residual modulation acts as noise (described in more detail  
217 below, Fig 4b). Finally, raw ANOVA values are biased by trial-by-trial variability (which the  
218 ANOVA addresses by computing the probability that each term is higher than chance given this  
219 noise) whereas our measures of modulation are bias-corrected to provide an unbiased estimate  
220 of modulation magnitude (see Methods).

221

222 Across the 235 IT units, we found that total nuisance modulation was larger than target match  
223 modulation in most cases (Fig 4a), and that average nuisance modulation was 2.7x the average  
224 target match signal (Fig 4b). A more detailed parsing of the total nuisance modulation into  
225 different subtypes revealed that the largest type of nuisance modulation could be attributed to  
226 "visual" modulations (on average 2.5x the target match signal; Fig 4b). Other types of  
227 modulation were also prominent, including "target" modulations (on average 0.8x the target  
228 match signal; Fig 4b), and "residual" modulation (on average 0.6x the target match modulation;  
229 Fig 4b). These results reveal that within IT, nuisance modulations are prominent and they are  
230 mixed with the target match signal in individual units.

231

232 In sum, the results presented thus far verify the existence of a robust, behaviorally-relevant  
233 target match signal in IT, and they confirm our predictions that IT target match signals are mixed  
234 with large nuisance modulations within individual IT units. Together, these results support  
235 assertions that the activity of IT units during visual target search should be an effective test of  
236 the impact that nuisance modulation has on neural task performance.

237



238 **Unexpectedly, the impact of nuisance modulation on single-unit performance is modest**

239

240 Ultimately, understanding the impact of nuisance modulation on linearly decoded task  
241 performance requires considering both the responses of individual units as well as their  
242 population interactions. Here we begin by quantifying the impact of nuisance modulation on  
243 individual units, the results of which were quite unexpected.

244

245 As a measure of linearly decoded target match performance for individual units, we focus on  
246 single-unit  $d'$  (Fig 1b). Single-unit  $d'$  is determined by the separation between the spike count  
247 responses of a unit to the set of all images presented as target matches versus the same  
248 images presented as distractors, and is quantified as the ratio between the distance between  
249 the means over the average standard deviation of the two distributions (Fig 1b). Single-unit  $d'$  is  
250 thus proportional to the amount of “target match signal”, equivalent to the distance between the  
251 means of the responses to target matches and to distractors (Fig 1b, cyan). Conversely, single-  
252 unit  $d'$  is inversely proportional to the spread within each distribution, where spread is  
253 determined by two factors. The first contributor to this spread is the variability in the spike count  
254 responses across repeated trials of the same condition, or “trial variability” (Fig 1b, purple). The  
255 second contributor to this spread is the dispersion between different conditions within each set,  
256 equivalent to all types of modulation that are not the target match signal (“nuisance” modulation;  
257 Fig 1b, red). This is why signal mixing is predicted to be detrimental to single-unit task  
258 performance – because any nuisance modulation that exists within a unit is predicted to  
259 increase the overlap between target matches and distractors.

260

261 In a previous report, we formalized these intuitions into a mathematical relationship between the  
262 single-unit modulation magnitudes as measured in Fig 4a-b and single-unit  $d'$  (Pagan and Rust,  
263 2014b). This derivation can be applied here with minor extensions. To summarize that  
264 approach,  $d'$  is a measure of the ratio between signal and noise, where signal is proportional to  
265 the amount of target match modulation (Fig 4b, cyan) and noise is parsed into one component  
266 proportional to total nuisance modulation (Fig 4b, red) and another component proportional to  
267 trial variability (Fig 4b, purple):

$$|d'| = \sqrt{\frac{k_1 * \text{target match modulation}^2}{k_2 * \text{nuisance modulation}^2 + \text{trial variability}^2}}$$

268 where  $k_1$  and  $k_2$  are constants (see Methods). With this formulation, the impact of nuisance  
269 modulation on  $d'$  can be determined by considering the increase in  $d'$  when nuisance modulation  
270 is incorporated into the calculation (i.e. for the intact data) compared to when it is not (i.e. a  
271 hypothetical scenario in which nuisance modulation does not exist, analogous to the increase in  
272  $d'$  in Fig 1a relative to 1b). Fig 4c shows the result of this analysis, which reveals that removing  
273 nuisance only results in a modest increase in  $d'$  across units, with an average increase of 8.6%.  
274 Focusing on the most informative units (i.e. those with the highest  $d'$ ), did not change the  
275 qualitative nature of the result (average impact for the top 25%, 15%, 10% of units = 9.8%, 9.3%  
276 and 9.3% respectively).

277

278 This modest increase was surprising in light of the fact that nuisance modulations were 2.7x the  
279 target match signal (Fig 4b, compare cyan and dark red bars), coupled with the intuition that  
280 large nuisance modulation should be highly detrimental to task performance (Fig 1b). However,  
281 this result can be understood by examining the trial variability component of the noise, which  
282 was even larger than the nuisance component (Fig 4b, compare red and purple bars) and as a  
283 result, dominated the denominator of the  $d'$  derivation. As an illustrative example, compare

284 ratios of the numbers  $5/(10+100)=0.045$  versus  $5/(0+100)=0.05$ ; while the first component of the  
285 denominator, 10, is 2-fold the size of the numerator (5), including versus excluding it only leads  
286 to a change in the total ratio of 10% because the denominator is dominated by the second entry,  
287 100. Consequently, although the amount of nuisance modulation is large relative to the size of  
288 the target match signal, its impact is blunted by the existence of trial variability, which is even  
289 larger. Stated differently, while IT nuisance modulations are larger than the IT target match  
290 signal, both are small relative to the size of trial variability. Because trial variability is so much  
291 larger than nuisance variability, the existence of nuisance modulation has little consequence for  
292  $d'$ .

293

### 294 **Large trial variability in IT is a consequence of fast processing**

295

296 Why is trial variability so much larger than nuisance modulation (and signal modulation) in our  
297 data? During the IDMS task, spike count windows were short, as a consequence of terminating  
298 the count window before the monkeys' reaction times, which were fast (Fig 2e; total counting  
299 window duration 170 ms, 80-250 ms following stimulus onset). Within these short spike count  
300 windows, the average grand mean spike count was 1 spike per condition per trial, and the  
301 average peak spike count across the 80 conditions was 2.77 spikes (which translates into mean  
302 and peak firing rates of 5.8 spikes/sec and 16.3 spikes/sec, respectively). We also found that,  
303 consistent with earlier reports, IT trial variability was approximately Poisson (average variance-  
304 to-mean ratio across units = 1.22, relative to the Poisson benchmark of 1.0). Simple simulations  
305 confirm that within a low spike count, Poisson regime, trial variability is much larger than signal  
306 modulation. Large trial variability in IT thus does not arrive from exotic mechanisms, rather, it is  
307 a natural consequence of the low spike counts that follow from fast processing, coupled with  
308 Poisson-like trial variability.

309

310 To illustrate how the impact of nuisance modulation depends on overall spike count, we  
311 recalculated the impact of nuisance modulation as a function of increasing window size. In this  
312 analysis, we always started the spike count window for each unit at 80 ms following stimulus  
313 onset, and we ended the count window at different times up to 170 ms total duration (equivalent  
314 to the count window for the analyses presented in Fig 4b-c). These results illustrate a  
315 systematic increase in the impact of nuisance modulation on task performance as a function of  
316 spike count window duration (Fig 4d), consistent with the interpretation that the impact of  
317 nuisance modulation is inversely proportional to the overall spike count.

318

319 To illustrate that the amount of signal mixing we observed would have impacted task  
320 performance at higher spike counts than we recorded in our data (e.g. if counting windows were  
321 longer and/or firing rates were higher), we performed a simulation in which we rescaled the  
322 responses for each unit in our data (after noise correction, see Methods). Specifically, we kept  
323 the proportions and types of signal and nuisance modulation for each unit intact, but rescaled  
324 the trial-averaged spike count responses for each unit by different factors of N, followed by the  
325 reintroduction of Poisson trial variability. We then recomputed the impact of nuisance  
326 modulation on single-unit  $d'$  as described for Fig 4c-d. We found that the impact of nuisance on  
327  $d'$  grew substantially with rescaling (Fig 5c). For example, with a 6-fold rescaling, which roughly  
328 translates into a 1 second counting window (under the assumption that the response properties  
329 are constant with time), eliminating nuisance resulted in a 50.2% increase in  $d'$  (as compared to  
330 the 11.7% increase in simulation with no rescaling). The increased impact of nuisance with  
331 rescaling cannot not be attributed to changes in the relative amounts of signal and nuisance  
332 modulation, as these remained fixed with rescaling (compare Fig 4b and 5b, cyan, red). Rather,

333 the increased impact of nuisance with rescaling is due to a decrease in magnitude of trial  
334 variability relative to the magnitudes of signal and nuisance modulation (compare Fig 4b and 5b,  
335 purple).

336  
337 Together, these results indicate that mixing signals in a fast processing regime (where spike  
338 counts are low) has the unexpected consequence that nuisance modulation is largely  
339 inconsequential for task performance. In contrast, our simulations reveal that mixing signals in  
340 the same proportions but in regime where spike counts are high (e.g. with long integration  
341 windows and/or higher firing rates) would be highly detrimental. These results thus suggest that  
342 within IT during the IDMS task, the potentially deleterious impact of nuisance modulation is  
343 blunted by virtue of a fast processing, low spike count regime.

344  
345  
346 ***The impact of nuisance modulation on population performance is also modest:***

347  
348 As we demonstrate in this section, the impact of nuisance modulation on IT performance  
349 described above for single units (Fig 4c), remains modest even when population factors are  
350 considered. To address population considerations, we begin with a data-based  
351 “pseudosimulation” approach that allows us to compute important benchmarks for our results.  
352 However, because these simulations require assumptions about the data, we also verify our  
353 results with analyses applied directly to neural data.

354  
355 To estimate the impact of nuisance modulation on IT population performance, we applied  
356 approach similar in concept to the single-unit analysis presented in Fig 4c, where we estimated  
357 the impact of nuisance by comparing the intact data with a hypothetical version of our data with  
358 nuisance removed. However, in the case of the population, we did not have an analytical  
359 solution and we thus performed pseudosimulations to determine it. To perform this analysis, we  
360 simulated the responses of two versions of each unit: an intact version with the same number  
361 and types of signals as well as the same grand mean spike count (after noise correction, see  
362 Methods), and a version in which the nuisance modulation was removed. In both cases, we  
363 simulated trial variability for each unit with independent, Poisson process. Cross-validated linear  
364 decoder performance, measured in units of population  $d'$ , grew within increasing population size  
365 for the intact and nuisance-removed populations with an approximately fixed ratio (Fig 6a).  
366 Consequently, the proportional impact of nuisance modulation as a function of population size  
367 took on a value of  $\sim 15\%$ , regardless of population size (Fig 6b, solid). These results suggest  
368 that the impact of nuisance modulation in our data is modest and does not depend on  
369 population size (under the assumption that trial variability is Poisson and is independent  
370 between units).

371  
372 Our simulation-based approach allowed us to estimate the impact of nuisance modulation on  
373 population performance relative to a benchmark of the same population but without nuisance.  
374 However, our pseudosimulations incorporate the assumption that trial variability is independent  
375 (i.e. uncorrelated) between units, whereas we do in fact expect it to be weakly correlated (e.g.  
376 Cohen and Maunsell, 2009). How might the existence of weakly correlated variability impact our  
377 results? To summarize the well-established framework for thinking about correlated trial  
378 variability (reviewed by Averbeck et al., 2006; Cohen and Kohn, 2011; Kohn et al., 2016), when  
379 the component of trial variability that falls along a linear decoding axis is uncorrelated between  
380 neurons, it will average away as a function of population size. Relative to this benchmark,  
381 correlated trial variability has the potential to either be beneficial or detrimental to performance



382 (Fig 7a). We have determined that nuisance modulation is similar insofar as the component of  
383 nuisance modulation that falls along a linear decoding axis that is uncorrelated between neurons  
384 will average away as a function of population size. Relative to this benchmark, interactions  
385 between neurons can configure nuisance modulation to have beneficial or detrimental  
386 consequences (Fig 7b).

387  
388 When a task does not include nuisance variability (e.g. a two-way discrimination between  
389 exactly two conditions), the impact of correlated trial variability on population performance can  
390 be measured by comparing performance for the simultaneously recorded, intact data with  
391 performance when the trials are independently shuffled for each unit to destroy correlations  
392 (Averbeck and Lee, 2006). Increases in performance with shuffling indicate that noise  
393 correlations are detrimental (Fig 7a, left) whereas decreases in performance indicate that noise  
394 correlations are beneficial (Fig 7a, right). This shuffling procedure can be extended for tasks that  
395 incorporate a nuisance component by comparing population performance for the intact data with  
396 performance when the experimental conditions are shuffled independently for each unit within  
397 each class (i.e. shuffling conditions within the set of target matches and within the set of  
398 distractors).

399  
400 To assess the impact of both correlated trial and nuisance variability on IT population  
401 performance, we analyzed the raw, simultaneously recorded data within each session. Here we  
402 present the results only for populations of size 24 (to simplify the data, given the number of  
403 comparisons of interest). Relative to the intact data, shuffling trial variability resulted in a small  
404 increase in performance (Fig 7c, “Intact” versus “Shuffle TV”; proportional increase with shuffling  
405 = 12%), indicating that correlated trial variability is aligned along the target match decoding axis  
406 in a manner that is weakly detrimental. Next we computed performance when both trial and  
407 nuisance variability were shuffled, and found that it was slightly higher than shuffling trial  
408 variability alone (Fig 7c, “Shuffle TV&NV”; proportional increase = 6%). This suggests that like  
409 trial variability, nuisance variability is correlated in a manner weakly detrimental to performance.

410  
411 How does the existence of weakly detrimental correlated trial and nuisance variability impact the  
412 results presented in Fig 6? First, note that the analysis presented in Fig 6 is not impacted by  
413 the existence of correlated trial variability (because any correlations were destroyed in the  
414 pseudosimulation process). Second, note that Fig 6 presents an estimate of the “total” impact of  
415 nuisance variability that captures contributions arising from both the existence of nuisance  
416 modulations as well as any detrimental correlations that fall along the decoding axis. To parse  
417 their relative contributions, we returned to the pseudosimulation and applied the nuisance  
418 shuffling procedure. Shuffling nuisance variability lead to a small proportional increase (relative  
419 to shuffling trial variability alone; Fig 7d; 5.4%) that was similar to the value measured for the  
420 intact data (6%, as described above). The proportional impact of removing nuisance variability  
421 altogether, after shuffling, was 9.4% (Fig 7d; “Shuffle&NV” vs. “Shuffle TV, Remove NV”).

422  
423 To summarize these results, we measured the impact of nuisance modulation on population  
424 performance in simulation by comparing performance of an intact population (with independent  
425 trial variability) with a simulation of the same population with nuisance variability removed. In our  
426 data, the impact of nuisance modulation was small (~15%) and approximately flat as a function  
427 of population size. An analysis targeted at understanding how correlated trial and nuisance  
428 variability between units impacts task performance revealed that their contributions to task  
429 performance were also measurable but modest, and did not change the interpretation that while

430 nuisance modulation is large in IT, its impact on task performance (both for single units and for  
431 the population) is small.

432

## 433 **Discussion:**

434

435 In many everyday situations, we are faced with the challenge of extracting one type of  
436 information from our environment while ignoring many other things that are going on around us.  
437 This study was inspired by a very simple intuition: when the neurons involved in computing the  
438 solutions for these tasks are modulated by both task-relevant signals as well as task-irrelevant  
439 nuisance information, nuisance modulation should be a source of noise that limits our ability to  
440 perform these tasks. Unexpectedly, we found that this simple intuition was largely wrong in IT.  
441 During a visual target search task, we found that nuisance modulations in IT were indeed large  
442 and that they were mixed with task-relevant signals in the responses of individual units,  
443 however, their consequences for task performance were modest. This result could be explained  
444 by the existence of another noise source, trial variability, which was larger than nuisance  
445 variability and blunted its impact on performance. Large trial variability in IT could, in turn, be  
446 accounted for by fast processing (implied by fast reaction times), which positioned IT within a  
447 low spike count regime, coupled with Poisson trial variability. We found that these results  
448 applied not only to individual units but also to the performance of the IT population. Our results  
449 thus reveal that when the brain operates in a regime where signals are small relative to the size  
450 of trial variability, nuisance modulations are of very little consequence to task performance.

451

452 Many of our intuitions about neural coding have been developed within the context of a high  
453 spike count regime, largely following on foundational work in early and mid-level visual brain  
454 areas in primates (e.g. V1, MT) where firing rates are high. Notably, recent work has called into  
455 question whether even in those brain areas, high spike counts do in fact translate into a high  
456 signal-to-noise ratio, due to supra-Poisson trial variability that begins to dominate when spike  
457 counts are large (Goris et al., 2014). Moreover, the low spike count regime that we present here  
458 is likely to be representative of the operating regime in many brain areas during many real-world  
459 tasks. The unexpected nature of our results highlights the fact that in this low spike count  
460 regime, some of the basic intuitions that we have constructed about neural coding may not hold.

461

462 Our results shed insight into why the brain might continue to “mix” modulations for different task-  
463 relevant parameters within individual neurons, even at the highest stages. Growing evidence  
464 suggests that the brain does not seek to produce neurons with increasingly “pure selectivity” at  
465 higher stages of processing, but rather that the brain continues to mix modulations for different  
466 task-relevant parameters within individual neurons, both at the locus at which task-relevant  
467 solutions are computed, as well as downstream (Freedman and Assad, 2009; Kobak et al.,  
468 2016; Mante et al., 2013; Meister et al., 2013; Raposo et al., 2014; Rigotti et al., 2013; Rishel et  
469 al., 2013; Zoccolan et al., 2007). A number of explanations have been proposed to account for  
470 mixed selectivity. Some studies have documented situations in which signal mixing is an  
471 inevitable consequence of the computations required for certain tasks, such as identifying  
472 objects invariant to the view in which they appear (Zoccolan et al., 2007). Others have  
473 suggested that mixed selectivity may be an essential component of the substrate required to  
474 maintain a representation that can rapidly and flexibly switch with changing task demands  
475 (Raposo et al., 2014; Rigotti et al., 2013). Still others have maintained that broad tuning across  
476 different types of parameters is important for learning new associations (Barak et al., 2013).  
477 When viewed from the perspective that signal mixing introduces noise in the form of nuisance

478 modulation, one might suspect that one or more of these benefits outweigh the performance  
479 costs associated with mixed selectivity. However as we demonstrate here, within the fast  
480 processing, low spike count regime that most of these high-level brain areas are likely to  
481 operate in, large nuisance modulations are expected to have only a modest impact on task  
482 performance.

483  
484 The framework with which we explore how nuisance interactions between different neurons  
485 impact population performance builds on foundational work focused on correlated trial variability  
486 between units, or “noise correlations” (Averbeck et al., 2006; Cohen and Kohn, 2011; Kohn et  
487 al., 2016). Recent work has emphasized the importance of not just measuring the degree to  
488 which neurons are correlated, but how those correlations align with a decoding axis and thus  
489 how they impact performance (Moreno-Bote et al., 2014). In the visual search task we present  
490 here, we found that correlations between units in both trial and nuisance variability had a small,  
491 detrimental impact on performance. In other tasks, nuisance interactions along a decoding axis  
492 may be much more impactful – such as in the case of dissociating self versus object motion  
493 (Kim et al., 2016), and in those cases, other decoding schemes may be required to  
494 disambiguate signal from nuisance modulation.

495  
496 Our results support the existence of a robust target match representation in IT during this task  
497 that reflects confusions on trials in which the monkeys make errors (Fig 3c); this result has not  
498 been reported previously. One earlier study also explored the responses of IT neurons in the  
499 context of a DMS task in which, like ours, the objects could appear at different identity-  
500 preserving transformations (Leuschow et al., 1994), but this study did not sort neural responses  
501 based on behavior. Target match signals have been investigated most extensively in IT via a  
502 classic version of the delayed-match-to-sample (DMS) paradigm where each trial begins with a  
503 visual cue indicating the identity of the target object, and this cue is often the same image as the  
504 target match. In this paradigm, approximately half of all IT neurons that differentiate target  
505 matches from distractors do so with enhanced responses to matches whereas the other half are  
506 match suppressed (Miller and Desimone, 1994; Pagan et al., 2013). Because match  
507 suppressed responses are thought to arise as the result of passive, stimulus repetition of the  
508 target match following the cue, some have speculated that the match enhanced neurons alone  
509 carry behaviorally-relevant target match information (Miller and Desimone, 1994). Conversely,  
510 others have argued that a representation comprised exclusively of match enhanced neurons  
511 would likely confuse the presence of a match with nuisance modulations that evoke changes in  
512 overall firing rate, such as changes in stimulus contrast (Engel and Wang, 2011). Additionally,  
513 these authors have proposed that matched suppressed neurons could be used in these cases  
514 to disambiguate target match versus nuisance modulation. Our results reveal that when target  
515 matches do not follow the presentation of the same visual image at a time short time before (as  
516 is the case for natural object search), match suppression is very weak (Fig 3e), and  
517 consequently, in these cases, this specific disambiguation strategy cannot be employed. Our  
518 results also suggest that for the types of nuisance modulation that we have investigated here  
519 (changes in position, size and background context), its impact is modest and in these cases,  
520 such a strategy is not necessary.

521  
522 In a previous series of reports (Pagan et al., 2013; Pagan and Rust, 2014a; Pagan et al., 2016),  
523 we investigated target match signals in the context of the classic DMS design in which target  
524 matches were repeats of cues presented earlier in the trial and each object was presented on a  
525 gray background. One of our main findings from that work was that the IT target match  
526 representation was reflected in a partially nonlinearly separable format, whereas an IT

527 downstream projection area, perirhinal cortex, contained the same amount of target match  
528 information but in a format that was largely linearly separable. In the data we present here, we  
529 also found evidence for a nonlinear component of the IT target match representation, reflected  
530 in the significantly higher performance of a maximum likelihood as compared to linear decoder  
531 (Fig 3b). However, in this study, a larger proportion of the IT target match representation was  
532 linear as compared to our previous DMS results. The source of these quantitative differences is  
533 unclear. They could arise from the fact that the IDMS task requires an “invariant” visual  
534 representation of object identity, which first emerges in a linearly separable format in the brain  
535 area that we are recording from (IT), whereas the DMS task could rely on the visual  
536 representation at an earlier stage. Alternatively, these differences could arise from the fact that  
537 during IDMS, images are not repeated within a trial, and the stronger nonlinear component  
538 revealed in DMS may be produced by stimulus repetition. Our current data cannot distinguish  
539 between these alternatives.

540

#### 541 **Acknowledgments**

542 We thank Marino Pagan for valuable insights, and Margot P. Wohl and Krystal Henderson for  
543 their technical contributions. This work was supported by the National Eye Institute of the US  
544 National Institutes of Health (award number R01EY020851).

545

#### 546 **Competing interests**

547 N.C.R. serves as a Board Review Editor for eLife.

548

## 549 **METHODS**

550

551 Experiments were performed on two adult male rhesus macaque monkeys (*Macaca mulatta*)  
552 with implanted head posts and recording chambers. All procedures were performed in  
553 accordance with the guidelines of the University of Pennsylvania Institutional Animal Care and  
554 Use Committee.

555

#### 556 **The invariant delayed-match-to-sample (IDMS) task:**

557

558 All behavioral training and testing was performed using standard operant conditioning (juice  
559 reward), head stabilization, and high-accuracy, infrared video eye tracking. Stimuli were  
560 presented on an LCD monitor with an 85 Hz refresh rate using customized software  
561 (<http://mworks-project.org>).

562

563 As an overview, the monkeys' task required an eye movement response to a specific location  
564 when a target object appeared within a sequence of distractor images (Fig 2a). Objects were  
565 presented across variation in the objects' position, size and background context (Fig 2b).  
566 Monkeys viewed a fixed set of 20 images across switches in the identity of 4 target objects,  
567 each presented at 5 identity-preserving transformations (Fig 2c). We ran the task in short blocks  
568 (~3 min) with a fixed target before another target was pseudorandomly selected. Our design  
569 included two types of trials: cue trials and test trials (Fig 2a). Only test trials were analyzed for  
570 this report.

571

572 Trials were initiated by the monkey fixating on a red dot ( $0.15^\circ$ ) in the center of a gray screen,  
573 within a square window of  $\pm 1.5^\circ$ , followed by a 250 ms delay before a stimulus appeared. Cue  
574 trials, which indicated the current target object, were presented at the beginning of each block

575 and after three subsequent trials with incorrect responses. To minimize confusion, cue trials  
576 were designed to be distinct from test trials and began with the presentation of an image of each  
577 object that was distinct from the images used on test trials (a large version of the object  
578 presented at the center of gaze on a gray background; Fig 2a). Test trials, which are the focus  
579 of this report, always began with a distractor image, and neural responses to this image were  
580 discarded to minimize non-stationarities such as stimulus onset effects. Distractors were drawn  
581 randomly from a pool of 15 possible images within each block without replacement until each  
582 distractor was presented once on a correct trial, and the images were then re-randomized. On  
583 most trials, a random number of 1-6 distractors were presented, followed by a target match (Fig  
584 2a). On a small fraction of trials, 7 distractors were shown, and the monkey was rewarded for  
585 fixating through all distractors. Each stimulus was presented for 400 ms (or until the monkeys'  
586 eyes left the fixation window) and was immediately followed by the presentation of the next  
587 stimulus. Following the onset of a target match image, monkeys were rewarded for making a  
588 saccade to a response target within a window of 75 – 600 ms to receive a juice reward. In  
589 monkey 1 this target was positioned 10 degrees below fixation; in monkey 2 it was 10 degrees  
590 above fixation. If 400 ms following target onset had elapsed and the monkey had not moved its  
591 eyes, a distractor stimulus was immediately presented. If the monkey continued fixating beyond  
592 the required reaction time, the trial was considered a “miss”. False alarms were differentiated  
593 from fixation breaks via a comparison of the monkeys' eye movements with the characteristic  
594 pattern of eye movements on correct trials: false alarms were characterized by the eyes leaving  
595 the fixation window via its bottom (monkey 1) or top (monkey 2) outside the allowable correct  
596 response period and traveling more than 0.5 degrees whereas fixation breaks were  
597 characterized by the eyes leaving the fixation window in any other way. Within each block, 4  
598 repeated presentations of the 20 images were collected, and a new target object was then  
599 pseudorandomly selected. Following the presentation of all 4 objects as targets, the targets  
600 were re-randomized. At least 20 repeats of each condition were collected. Overall, monkeys  
601 performed this task with high accuracy. Disregarding fixation breaks (monkey 1: 8% of trials,  
602 monkey 2: 12% of trials), percent correct on the remaining trials was as follows: monkey 1: 87%  
603 correct, 3% false alarms, and 10% misses; monkey 2: 97% correct, <1% false alarms, and 3%  
604 misses.

### 605 606 **Neural recording:**

607  
608 The activity of neurons in IT was recorded via a single recording chamber in each monkey.  
609 Chamber placement was guided by anatomical magnetic resonance images in both monkeys,  
610 and in one monkey, Brainsight neuronavigation (<https://www.rogue-research.com/>). The region  
611 of IT recorded was located on the ventral surface of the brain, over an area that spanned 4 mm  
612 lateral to the anterior middle temporal sulcus and 15-19 mm anterior to the ear canals. Neural  
613 activity was largely recorded with 24-channel U probes (Plexon, Inc) with linearly arranged  
614 recording sites spaced with 100  $\mu\text{m}$  intervals, with a handful of units recorded with single  
615 electrodes (Alpha Omega, glass-coated tungsten). Continuous, wideband neural signals were  
616 amplified, digitized at 40 kHz and stored using the OmniPlex Data Acquisition System (Plexon).  
617 Spike sorting was done manually offline (Plexon Offline Sorter). At least one candidate unit was  
618 identified on each recording channel, and 2-3 units were occasionally identified on the same  
619 channel. Spike sorting was performed blind to any experimental conditions to avoid bias. The  
620 sample size (number of units recorded) was chosen to approximately match our previous work  
621 (Pagan et al., 2013; Pagan and Rust, 2014a; Pagan et al., 2016).

622  
623 For all the analyses presented in this paper, we measured neural responses by counting spikes



624 in a window that began 80 ms after stimulus onset. For all analyses but Fig 4d, the spike count  
625 window ended at 250 ms. On 2.0% of all correct target match presentations, the monkeys had  
626 reaction times faster than 250 ms, and those instances were excluded from analysis such that  
627 spikes were only counted during periods of fixation. When combining the units recorded across  
628 sessions into a larger pseudopopulation, we screened for units that met three criteria. First, units  
629 had to be modulated by our task, as quantified by a one-way ANOVA applied to our neural  
630 responses (80 conditions \* 20 repeats) with  $p < 0.01$ . Second, we applied a loose criterion on  
631 recording stability, as quantified by calculating the variance-to-mean for each unit (computed by  
632 fitting the relationship between the mean and variance of spike count across the 80 conditions),  
633 and eliminating units with a variance-to-mean ratio  $> 5$ . Finally, we applied a loose criterion on  
634 unit recording isolation, quantified by calculating the signal-to-noise ratio (SNR) of the waveform  
635 (as the difference between the maximum and minimum points of the average waveform, divided  
636 by twice the standard deviation across the differences between each waveform and the mean  
637 waveform), and excluding (multi)units with an SNR  $< 2$ . This yielded a pseudopopulation of 235  
638 units (of 589 possible units), including 99 units from monkey 1 and 126 units from monkey 2.

639

#### 640 **Population performance:**

641

642 To determine the performance of the IT population at classifying target matches versus  
643 distractors, we applied two types of decoders: a Fisher Linear Discriminant (a linear decoder)  
644 and Maximum Likelihood decoder (a nonlinear decoder) using approaches described previously  
645 in detail (Pagan et al., 2013) and are summarized here.

646

647 When applied to the pseudopopulation data (Fig 3b, Fig 6a), all decoders were cross-validated  
648 with the same resampling procedure. On each iteration of the resampling, we randomly shuffled  
649 the trials for each condition and for each unit, and (for numbers of neurons less than the full  
650 population size) randomly selected units. On each iteration, 18 trials from each condition were  
651 used for training the decoder, 1 trial was used to determine a value for regularization, and 1 trial  
652 from each condition was used for cross-validated measurement of performance.

653

654 To ensure that decoder performance was not biased by unequal numbers of target matches and  
655 distractors, on each iteration of the resampling we included 20 target match conditions and 20  
656 (of 60 possible) distractor conditions. Each set of 20 distractors was selected to span all  
657 possible combinations of mismatched object and target identities (e.g. objects 1, 2, 3, 4 paired  
658 with targets 4, 3, 2, 1), of which there are 9 possible sets. When computing proportion correct  
659 (Fig 3b), a mean performance value was computed on each resampling iteration by averaging  
660 binary performance outcomes across the 9 possible sets of target matches and distractors,  
661 each which contained 40 test trials. Mean and standard error of performance was computed as  
662 the mean and standard deviation of performance across 2000 resampling iterations. When  
663 computing population  $d'$  (Fig 6a),  $d'$  was computed on each resampling iteration for the 20 target  
664 match conditions and 20 distractor conditions, separately for each set of 9 match/distractor  
665 combinations, and then averaged across the 9 sets. Mean and standard error of population  $d'$   
666 was computed as the mean and standard deviation of  $d'$  across 2000 resampling iterations. For  
667 both measures, standard error thus reflected the variability due to the specific trials assigned to  
668 training and testing and, for populations smaller than the full size, the specific units chosen.

669

670

671

672 *Fisher Linear Discriminant:*

673

674 The general form of a linear decoding axis is:

675

676 (1)  $f(x) = \mathbf{w}^T \mathbf{x} + b$ ,

677

678 where  $\mathbf{w}$  is an N-dimensional vector (where N is the number of units) containing the linear  
679 weights applied to each unit, and  $b$  is a scalar value. We fit these parameters using a Fisher  
680 Linear Discriminant (FLD), where the vector of linear weights was calculated as:

681

682 (2)  $\mathbf{w} = \Sigma^{-1}(\mu_1 - \mu_2)$

683

684 and  $b$  was calculated as:

685

686 (3)  $b = \mathbf{w} \cdot \frac{1}{2}(\mu_1 + \mu_2) = \frac{1}{2}\mu_1^T \Sigma^{-1} \mu_1 - \frac{1}{2}\mu_2^T \Sigma^{-1} \mu_2$

687

688 Here  $\mu_1$  and  $\mu_2$  are the means of the two classes (target matches and distractors, respectively)  
689 and the mean covariance matrix is calculated as:

690

691 (4)  $\Sigma = \frac{\Sigma_1 + \Sigma_2}{2}$

692

693 where  $\Sigma_1$  and  $\Sigma_2$  are the regularized covariance matrices of the two classes. These covariance  
694 matrices were computed using a regularized estimate equal to a linear combination of the  
695 sample covariance and the identity matrix  $I$  (Pagan et al., 2016):

696

697 (5)  $\Sigma_i = \gamma \Sigma_i + (1 - \gamma) \cdot I$

698

699 To maintain consistency across the different analyses presented throughout the paper, we fixed  
700  $\gamma$  to be 0.9 for all analyses. We determined this value by exploring a range of different  $\gamma$ , and  
701 selecting the value that maximized performance globally. Results were qualitatively similar  
702 across a range of  $\gamma$ . In this calculation of the FLD parameters, both the information conveyed by  
703 individual units as well as their pairwise interactions are considered.

704

705 We computed two measures of performance: proportion correct (Fig 3b-c), and population  $d'$   
706 (Fig 6a). Each calculation began by computing the dot product of the test data and the linear  
707 weights  $\mathbf{w}$ , adjusted by  $b$  (Eq. 1). Proportion correct was computed as the fraction of test trials  
708 that were correctly assigned as target matches and distractors, according to their true labels.  
709 Population  $d'$  was computed for the distributions of these values across the 20 different images  
710 presented as target matches versus as distractors:

711

712 (6)  $d' = \frac{|\mu_{Match} - \mu_{Distractor}|}{\sigma_{pooled}}$ ,

713

714 where  $\mu_{Match}$  and  $\mu_{Distractor}$  correspond to the mean across the set of matches and distractors,

715  $\sigma_{pooled} = \sqrt{\frac{\sigma_{Match}^2 + \sigma_{Distractor}^2}{2}}$ , and  $\sigma_{Match}$  and  $\sigma_{Distractor}$  correspond to the standard deviation

716 across the set of matches and distractors, respectively.

717

718 To compare FLD performance on correct versus error trials (Fig 3c), we used the same methods  
719 described above with the following modifications. First, the analysis was applied to the  
720 simultaneously recorded data within each session, and the correlation structure on each trial  
721 was kept intact on each resampling iteration. Second, when more than 24 units were available,  
722 a subset of 24 units were selected as those with the most task modulation, quantified via the p-  
723 value of a one-way ANOVA applied to each unit's responses (80 conditions \* 20 repeats).  
724 Finally, on each resampling iteration, each error trial was randomly paired with a correct trial of  
725 the same condition and cross-validated performance was performed exclusively for these pairs  
726 of correct and error responses. As was the case for the pseudopopulation analysis, training  
727 was performed exclusively on correct trials. A mean performance value was computed on each  
728 resampling iteration by averaging binary performance outcomes across all possible error trials  
729 and their condition-matched correct trial pairs, and averaging across different recording  
730 sessions. Mean and standard error of performance was computed as the mean and standard  
731 deviation of performance across 2000 resampling iterations. Standard error thus reflected error  
732 in a manner similar to the pseudopopulation analysis - the variability due to the specific trials  
733 assigned to training and testing and, for populations smaller than the full size, the specific units  
734 chosen.

735  
736 To determine the impact of correlated trial and nuisance variability on IT population performance  
737 (Fig 7c-d), we compared the FLD applied to the simultaneously recorded data as described  
738 above where the correlation structure on each trial was kept intact on each resampling iteration  
739 (Fig 7c, "intact"), with two different shuffling procedures. In the first, we randomly shuffled the  
740 trials within each condition, for each unit, on each iteration of the bootstrap (Fig 7c, "Shuffle  
741 TV"). In the second, we randomly shuffled both trial variability as well as the order of assignment  
742 of each the 20 distractor conditions and 20 target match conditions on each bootstrap iteration  
743 (Fig 7c & 7d, "Shuffle TV & NV").

744  
745 *Maximum likelihood decoder:*

746  
747 As a measure of total IT target match information (combined linear and nonlinear), we  
748 implemented a maximum likelihood decoder (Fig 3b). We began by using the set of training  
749 trials to compute the average response  $r_{uc}$  of each unit  $u$  to each of the 40 conditions  $c$ . We then  
750 computed the likelihood that a test response  $k$  was generated from a particular condition as a  
751 Poisson-distributed variable:

752  
753 
$$(7) \text{lik}_{u,c}(k) = \frac{(r_{uc})^k \cdot e^{-r_{uc}}}{k!}$$

754  
755 The likelihood that a population response vector was generated in response to each condition  
756 was then computed as the product of the likelihoods of the individual neurons. Next, the  
757 likelihood that each test vector arose from the category target match as compared to the  
758 category distractor as the product of the likelihoods across the conditions within each category.  
759 We assigned the population response to the category with the maximum likelihood, and we  
760 computed performance as the fraction of trials in which the classification was correct based on  
761 the true labels of the test data.

762  
763  
764  
765

## 766 **Quantifying single-unit modulation magnitudes:**

767

768 To quantify the degree to which the firing rates of individual units were modulated by whether an  
769 image was presented as a target match versus as a distractor (Fig 3d), we calculated a target  
770 match modulation index for each unit by computing its mean spike count response to target  
771 matches and to distractors, and computing the ratio of their difference and their sum.

772 To quantify the degree to which individual units were modulated by different types of task  
773 parameters, we applied a bias-corrected, ANOVA-like procedure described in detail by (Pagan  
774 et al., 2016) and summarized here. As an overview, this procedure considers the total variance  
775 in the spike count responses for each unit across conditions ( $n=80$ ) and trials for each condition  
776 ( $m=20$ ), and parses this total variance into the variance that can be attributed to each type of  
777 experimental parameter and variance attributed to trial variability. Like an ANOVA, the  
778 procedure is designed to parse response variance in an intuitive way, such as the variance that  
779 can be attributed to changes in the identity of the visual image, the identity of the target object  
780 and whether each condition was a target match or a distractor. These variances are converted  
781 into measures of spike count modulation (i.e. standard deviation around each unit's grand mean  
782 spike count) via a procedure that includes bias correction for over-estimates in modulation due  
783 to noise.

784

785 The procedure begins by developing an orthonormal basis of 80 vectors designed to capture all  
786 types of modulation with intuitive groupings. The number of each type is imposed by the  
787 experimental design. This basis  $\mathbf{b}$  included vectors  $\mathbf{b}_i$  that reflected 1) the grand mean spike  
788 count across all conditions ( $\mathbf{b}_1$ , 1 dimension), 2) whether the object in view was a target or a  
789 distractor ( $\mathbf{b}_2$ , 1 dimension), 3) visual image identity ( $\mathbf{b}_3 - \mathbf{b}_{21}$ , 19 dimensions), 4) target object  
790 identity ( $\mathbf{b}_{22} - \mathbf{b}_{24}$ , 3 dimensions), and 5) "residual", nonlinear interactions between target and  
791 object identity not captured by target match modulation ( $\mathbf{b}_{25} - \mathbf{b}_{80}$ , 56 dimensions). A Gram-  
792 Schmidt process was used to convert an initially designed set of vectors into an orthonormal  
793 basis.

794

795 Because this basis spans the space of all possible responses for our task, each trial-averaged  
796 vector of spike count responses to the 80 experimental conditions  $\mathbf{R}$  can be re-expressed as a  
797 weighted sum of these basis vectors. To quantify the amounts of each type of modulation  
798 reflected by each unit, we began by computing the squared projection of each basis vector  
799  $\mathbf{b}_i$  and  $\mathbf{R}$ . An analytical bias correction was then subtracted from this value (Pagan and Rust,  
800 2014b):

801

$$802 \quad (8) \quad w_i^2 = (\mathbf{R} \cdot \mathbf{b}_i^T)^2 - \frac{\sigma_t^2 \cdot (\mathbf{b}_i^T)^2}{m}$$

803

804 where  $\sigma_t^2$  indicates the trial variance, averaged across conditions ( $n=80$ ), and where  $m$  indicates  
805 the number of trials ( $m=20$ ). When more than one dimension existed for a type of modulation,  
806 we summed values of the same type. Next, we applied a normalization factor ( $1/(n-1)$  where  
807  $n=80$ ) to convert these summed values into variances. Finally, we computed the square root of  
808 these quantities to convert them into modulation units that reflected the number of spike count  
809 standard deviations around each unit's grand mean spike count. Target match modulation was  
810 thus computed as:

811

$$812 \quad (9) \quad \sigma_{TM} = \sqrt{\frac{1}{n-1} \cdot w_2^2}$$

813  
814 and nuisance modulation was computed as:  
815

$$816 \quad (10) \quad \sigma_{Nui} = \sqrt{\frac{1}{n-1} \cdot \sum_{i=3}^{80} w_i^2}$$

817  
818 Similarly, to compute the different subtypes of nuisance modulation, we replaced the weights  $w_i^2$   
819 in Eq. 10 with the weights that corresponded to the orthonormal basis vectors corresponding to  
820 each subtype, including visual modulation ( $i = 3$  to  $21$ ), target modulation ( $i = 22$  to  $24$ ), and 3  
821 residual modulation ( $i = 25$  to  $80$ ), as described above.  
822

823 We computed the trial variability for each unit ( $\sigma_{Trial}$ ) in a comparable manner as the square  
824 root of the average (across conditions) variance across trials:

$$825 \quad (11) \quad \sigma_{Trial} = \sqrt{\frac{1}{n} \cdot \sum_{i=1}^n \frac{1}{m-1} \cdot \sum_{t=1}^m (s_{it} - s_i)^2}$$

826  
827 where the spike count response for a particular trial  $t$  of condition  $i$  was  $s_{it}$ , and the mean spike  
828 count response across all trials of condition  $i$  was  $s_i$ .  
829  
830

831 When estimating modulation for individual units, (Fig 4a), the bias-corrected squared values  
832 were rectified for each unit before taking the square root. When estimating modulation  
833 population means (Fig 4b, 5b), the bias-corrected squared values were averaged across units  
834 before taking the square root. Because these measures were not normally distributed, standard  
835 error about the mean was computed via a bootstrap procedure. On each iteration of the  
836 bootstrap (across 1000 iterations), we randomly sampled values from the modulation values for  
837 each unit in the population, with replacement. Standard error was computed as the standard  
838 deviation across the means of these newly created populations.  
839

#### 840 **Relating modulation magnitudes and single unit performance ( $d'$ ):**

841  
842 To determine the impact of nuisance modulation on single unit task performance (Fig 4c-d, Fig  
843 5a) we re-expressed  $d'$  (Eq. 6) as a function of the different types of signal modulations  
844 described above (Eqs. 8-10):  
845

$$846 \quad (12) \quad d' = \frac{|\mu_{Match} - \mu_{Distractor}|}{\sigma_{pooled}} = \sqrt{\frac{a \cdot \sigma_M^2}{b \cdot \sigma_{Nui}^2 + \sigma_{Trial}^2}} \text{ where } a = \frac{n-1}{3}, \text{ and } b = \frac{n-1}{n}$$

847  
848 This derivation is described in detail in Pagan & Rust (2014).  
849

850 To quantify the impact of nuisance modulation on single unit performance ( $d'$ ), we compared  
851 each unit's  $d'$  in the presence of nuisance modulation (Eq. 12) versus  $d'$  when the nuisance  
852 modulation term  $\sigma_{Nui}$  was set to zero ( $d'_{NoNui}$ ). We then calculated the impact of nuisance  
853 modulation as the percent increase in  $d'$  without nuisance:  
854

$$855 \quad (13) \quad Impact = \left( \frac{d'}{d'_{NoNui}} - 1 \right) \cdot 100\%$$

856



857  
858  
859  
860  
861  
862  
863  
864  
865  
866  
867  
868  
869  
870  
871  
872  
873  
874  
875  
876  
877  
878

## **Simulations:**

To better understand our results, we performed a number of data-inspired simulations. Each simulation began by computing the bias-corrected weights for each unit as described above (Eq. 8).

To explore how rescaling the spike counts by different factors of  $N$  influenced the impact of nuisance modulation (Fig 5), we rectified bias-corrected modulations that fell below zero, recomputed the noise-corrected mean spike count responses for each condition, rescaled the mean spike counts by  $N$ , and generated trial variability with an independent Poisson process.

To estimate the impact of nuisance modulation on population performance, we simulated two versions of each of our recorded units (Fig 6a compare “Intact” to “Nuisance removed”; Fig 7d compare “Shuffle TV” and “Shuffle TV & NV” to “Shuffle TV, remove NV”). In the “Intact” version, we computed each unit’s responses as described for the rescaling simulation but with a rescale factor  $N = 1$ . In the “Nuisance removed” version, we used a similar procedure but set the modulations corresponding to all nuisance dimensions to zero. The responses were thus computed based on the grand mean spike count response as well as the target match modulation alone.

879 **References:**

880

881 Averbeck, B.B., Latham, P.E., and Pouget, A. (2006). Neural correlations, population coding and  
882 computation. *Nat Rev Neurosci* 7, 358-366.

883 Averbeck, B.B., and Lee, D. (2006). Effects of noise correlations on information encoding and  
884 decoding. *J Neurophysiol* 95, 3633-3644.

885 Barak, O., Rigotti, M., and Fusi, S. (2013). The sparseness of mixed selectivity neurons controls  
886 the generalization-discrimination trade-off. *J Neurosci* 33, 3844-3856.

887 Chelazzi, L., Miller, E.K., Duncan, J., and Desimone, R. (1993). A neural basis for visual search  
888 in inferior temporal cortex. *Nature* 363, 345-347.

889 Cohen, M.R., and Kohn, A. (2011). Measuring and interpreting neuronal correlations. *Nat*  
890 *Neurosci* 14, 811-819.

891 Cohen, M.R., and Maunsell, J.H. (2009). Attention improves performance primarily by reducing  
892 interneuronal correlations. *Nat Neurosci* 12, 1594-1600.

893 DiCarlo, J.J., and Cox, D.D. (2007). Untangling invariant object recognition. *Trends Cogn Sci* 11,  
894 333-341.

895 Engel, T.A., and Wang, X.J. (2011). Same or different? A neural circuit mechanism of similarity-  
896 based pattern match decision making. *J Neurosci* 31, 6982-6996.

897 Eskandar, E.N., Optican, L.M., and Richmond, B.J. (1992). Role of inferior temporal neurons in  
898 visual memory. II. Multiplying temporal waveforms related to vision and memory. *J Neurophysiol*  
899 68, 1296-1306.

900 Freedman, D.J., and Assad, J.A. (2009). Distinct encoding of spatial and nonspatial visual  
901 information in parietal cortex. *J Neurosci* 29, 5671-5680.

902 Goris, R.L., Movshon, J.A., and Simoncelli, E.P. (2014). Partitioning neuronal variability. *Nat*  
903 *Neurosci* 17, 858-865.

904 Haefner, R.M., and Bethge, M. (2010). Evaluating neural codes for inference using Fisher  
905 Information. Paper presented at: Advances in Information Processing Systems.

906 Hong, H., Yamins, D.L., Majaj, N.J., and DiCarlo, J.J. (2016). Explicit information for category-  
907 orthogonal object properties increases along the ventral stream. *Nat Neurosci* 19, 613-622.

908 Hung, C.P., Kreiman, G., Poggio, T., and DiCarlo, J.J. (2005). Fast readout of object identity  
909 from macaque inferior temporal cortex. *Science* 310, 863-866.

910 Kim, H.R., Pitkow, X., Angelaki, D.E., and DeAngelis, G.C. (2016). A simple approach to  
911 ignoring irrelevant variables by population decoding based on multisensory neurons. *J*  
912 *Neurophysiol* 116, 1449-1467.

- 913 Kobak, D., Brendel, W., Constantinidis, C., Feierstein, C.E., Kepecs, A., Mainen, Z.F., Qi, X.L.,  
914 Romo, R., Uchida, N., and Machens, C.K. (2016). Demixed principal component analysis of  
915 neural population data. *Elife* 5.
- 916 Kohn, A., Coen-Cagli, R., Kanitscheider, I., and Pouget, A. (2016). Correlations and Neuronal  
917 Population Information. *Annu Rev Neurosci* 39, 237-256.
- 918 Kosai, Y., El-Shamayleh, Y., Fyall, A.M., and Pasupathy, A. (2014). The role of visual area V4 in  
919 the discrimination of partially occluded shapes. *J Neurosci* 34, 8570-8584.
- 920 Leuschow, A., Miller, E.K., and Desimone, R. (1994). Inferior temporal mechanisms for invariant  
921 object recognition. *Cerebral Cortex* 5, 523-531.
- 922 Li, N., Cox, D.D., Zoccolan, D., and DiCarlo, J.J. (2009). What response properties do individual  
923 neurons need to underlie position and clutter "invariant" object recognition? *J Neurophysiol* 102,  
924 360-376.
- 925 Mante, V., Sussillo, D., Shenoy, K.V., and Newsome, W.T. (2013). Context-dependent  
926 computation by recurrent dynamics in prefrontal cortex. *Nature* 503, 78-84.
- 927 Maunsell, J.H., Sclar, G., Nealey, T.A., and DePriest, D.D. (1991). Extraretinal representations  
928 in area V4 in the macaque monkey. *Vis Neurosci* 7, 561-573.
- 929 Meister, M.L., Hennig, J.A., and Huk, A.C. (2013). Signal multiplexing and single-neuron  
930 computations in lateral intraparietal area during decision-making. *J Neurosci* 33, 2254-2267.
- 931 Miller, E.K., and Desimone, R. (1994). Parallel Neuronal Mechanisms for Short-Term-Memory.  
932 *Science* 263, 520-522.
- 933 Moreno-Bote, R., Beck, J., Kanitscheider, I., Pitkow, X., Latham, P., and Pouget, A. (2014).  
934 Information-limiting correlations. *Nat Neurosci* 17, 1410-1417.
- 935 Pagan, M., L.S., U., M.P., W., and Rust, N.C. (2013). Signals in inferotemporal cortex and  
936 perirhinal cortex suggest an untangling of visual target information. *Nature Neuroscience* 16,  
937 1132-1139.
- 938 Pagan, M., and Rust, N.C. (2014a). Dynamic target match signals in perirhinal cortex can be  
939 explained by instantaneous computations that act on dynamic input from inferotemporal cortex.  
940 *J Neurosci* 34, 11067-11084.
- 941 Pagan, M., and Rust, N.C. (2014b). Quantifying the signals contained in heterogeneous neural  
942 responses and determining their relationships with task performance. *J Neurophysiol* 112, 1584-  
943 1598.
- 944 Pagan, M., Simoncelli, E.P., and Rust, N.C. (2016). Neural Quadratic Discriminant Analysis:  
945 Nonlinear Decoding with V1-Like Computation. *Neural Comput*, 1-29.
- 946 Raposo, D., Kaufman, M.T., and Churchland, A.K. (2014). A category-free neural population  
947 supports evolving demands during decision-making. *Nat Neurosci* 17, 1784-1792.

- 948 Rigotti, M., Barak, O., Warden, M.R., Wang, X.J., Daw, N.D., Miller, E.K., and Fusi, S. (2013).  
949 The importance of mixed selectivity in complex cognitive tasks. *Nature* 497, 585-590.
- 950 Rishel, C.A., Huang, G., and Freedman, D.J. (2013). Independent category and spatial  
951 encoding in parietal cortex. *Neuron* 77, 969-979.
- 952 Rust, N.C., and DiCarlo, J.J. (2010). Selectivity and tolerance ("invariance") both increase as  
953 visual information propagates from cortical area V4 to IT. *J Neurosci* 30, 12978-12995.
- 954 Zoccolan, D., Kouh, M., Poggio, T., and DiCarlo, J.J. (2007). Trade-off between object  
955 selectivity and tolerance in monkey inferotemporal cortex. *J Neurosci* 27, 12292-12307.  
956

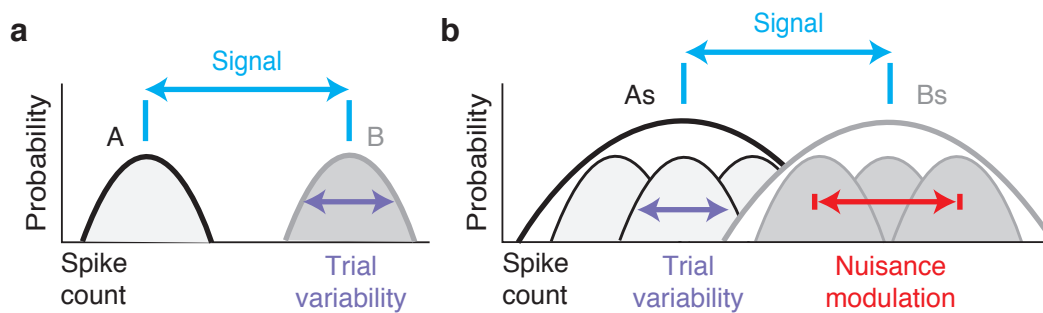




**Figure 1. Nuisance modulation limits task performance.** **a)** Schematic of single unit task performance ( $d'$ ) for a classic, two-way discrimination task in which a subject is asked to label different conditions as “A” or “B” across repeated trials. Shown are hypothetical distributions of spike count responses for the two conditions. Neural task performance,  $d'$ , is measured as the separation of the two spike count distributions in units of the number of standard deviations separating their means.  $d'$  is proportional to the amount of signal, which determines the separation between the means of the distributions (cyan), and  $d'$  is inversely proportional to spread within each distribution, which arises as a result of variability across repeated trials within each condition (“trial variability”; purple). **b)** Schematic of single unit task performance ( $d'$ ) for the same discrimination task, but extended to require grouping multiple conditions into each of two sets, “As” and “Bs” (e.g. an object identification task where two objects are presented in multiple background contexts). In this case, “nuisance” modulations (e.g. firing modulations by the background context), increase the spread of the responses within each condition and thus lower  $d'$ .

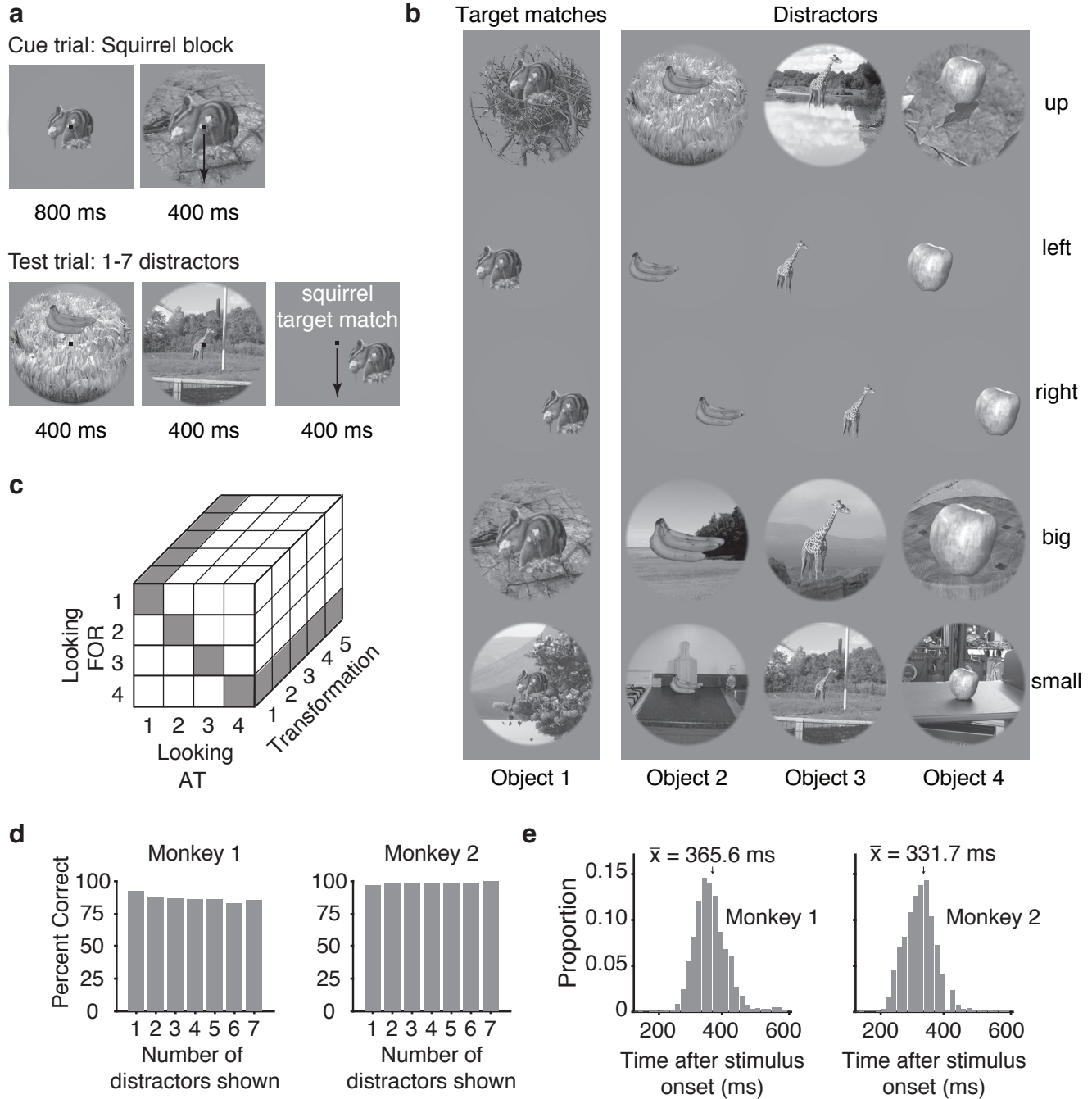


**Figure 2.** *The invariant delayed-match-to-sample task.* **a)** Monkeys performed an invariant delayed-match-to-sample task. Each block (~3 minutes in duration) began with a cue trial indicating the target object for that block. On subsequent trials, monkeys initiated a trial by fixating on a small dot. After a 250 ms delay, a random number (1-7) of distractors were presented, and on most trials, this was followed by the target match. Monkeys were required to maintain fixation throughout the distractors and make a saccade to a response dot within a window 75 - 600 ms following the onset of the target match to receive a reward. In cases where the target match was presented for 400 ms and the monkey had still not broken fixation, a distractor stimulus was immediately presented. **b)** The experiment included 4 objects presented at each of 5 identity-preserving transformations (“up”, “right”, “left”, “big”, “small”), for 20 images in total. In any given block, 5 of the images were presented as target matches and 15 were distractors. **c)** The complete experimental design included looking “at” each of 4 objects, each presented at 5 identity-preserving transformations (for 20 images in total), viewed in the context of looking “for” each object as a target. In this design, target matches (highlighted in gray) fall along the diagonal of each “looking at” / “looking for” transformation slice. **d)** Percent correct for each monkey, calculated based on both misses and false alarms (but disregarding fixation breaks). Percent correct is plotted as a function of the number of distractors shown. **e)** Histograms of reaction times during correct trials (ms after stimulus onset) during the IDMS task for each monkey, with means indicated by arrows and labeled.

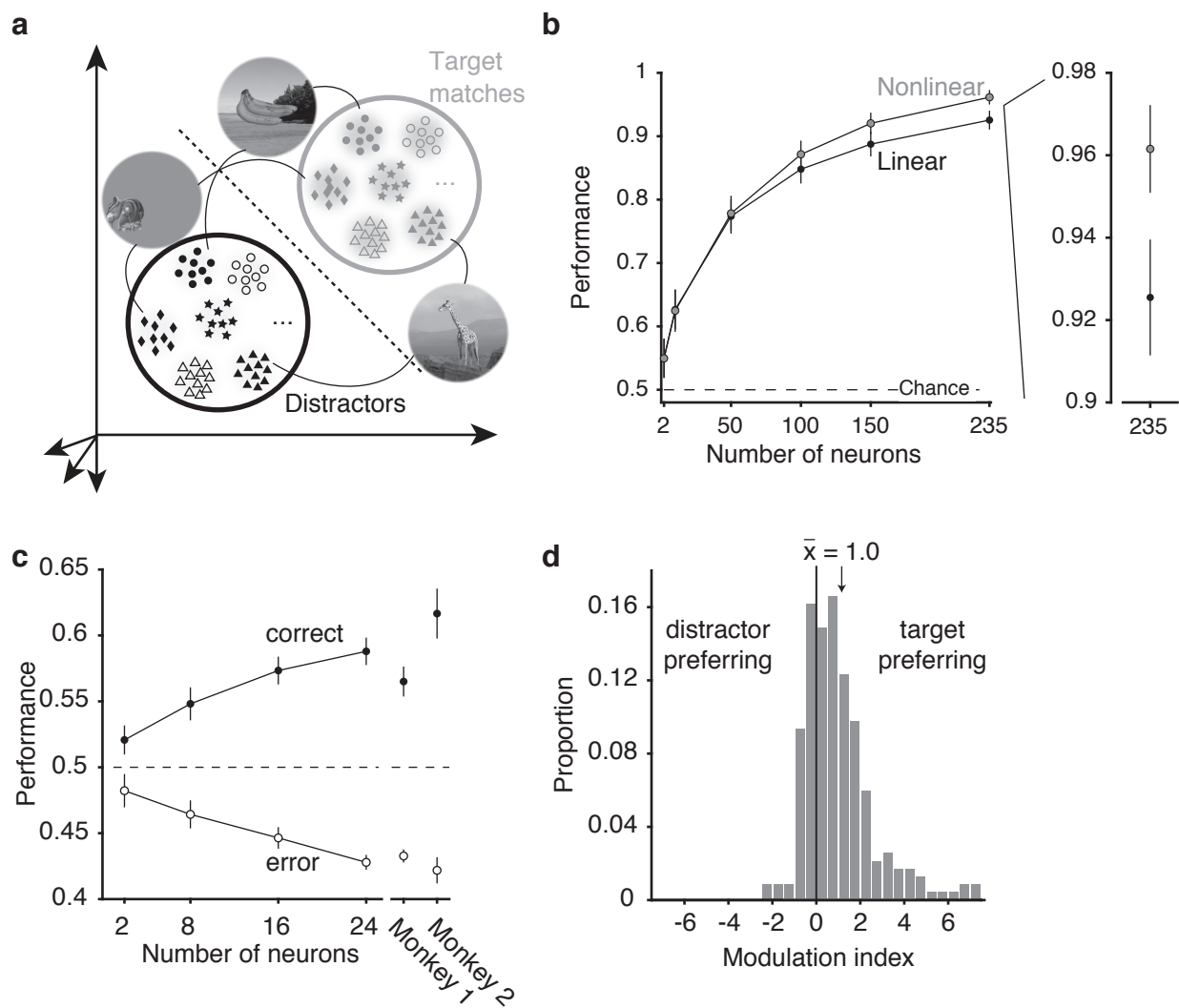


**Figure 3.** *IT reflects behaviorally-relevant target match information during the IDMS task.* **a)** The target search task can be envisioned as a two-way classification of the same images presented as target matches versus as distractors. Shown are cartoon depictions where each point depicts a hypothetical population response for a population of two neurons on a single trial, and clusters of points depict the dispersion of responses across repeated trials for the same condition. Included are responses to the same images presented as target matches and as distractors - here only 6 images are depicted but 20 images were used in the actual analysis. The dotted line depicts a hypothetical linear decision. **b)** Linear (FLD) and nonlinear (maximum likelihood) decoder performance as a function of population size for a pseudopopulation of 235 units. Error bars (SEM) reflect the variability that can be attributed to the random selection of units (for populations smaller than the full dataset) and the random assignment of training and testing trials in cross-validation. **c)** Linear decoder performance, for simultaneously recorded data, after training on correct trials and cross-validating on pairs of correct and error trials matched for condition. Error bars (SEM) reflect the variability that can be attributed to the random selection of units (for populations smaller than the full dataset) and the random assignment of training and testing trials in cross-validation. **d)** A match modulation index, computed for each unit by calculating the mean spike count response to target matches and to distractors, and computing the ratio of the difference and the sum of these two values. Arrow indicates the distribution mean.

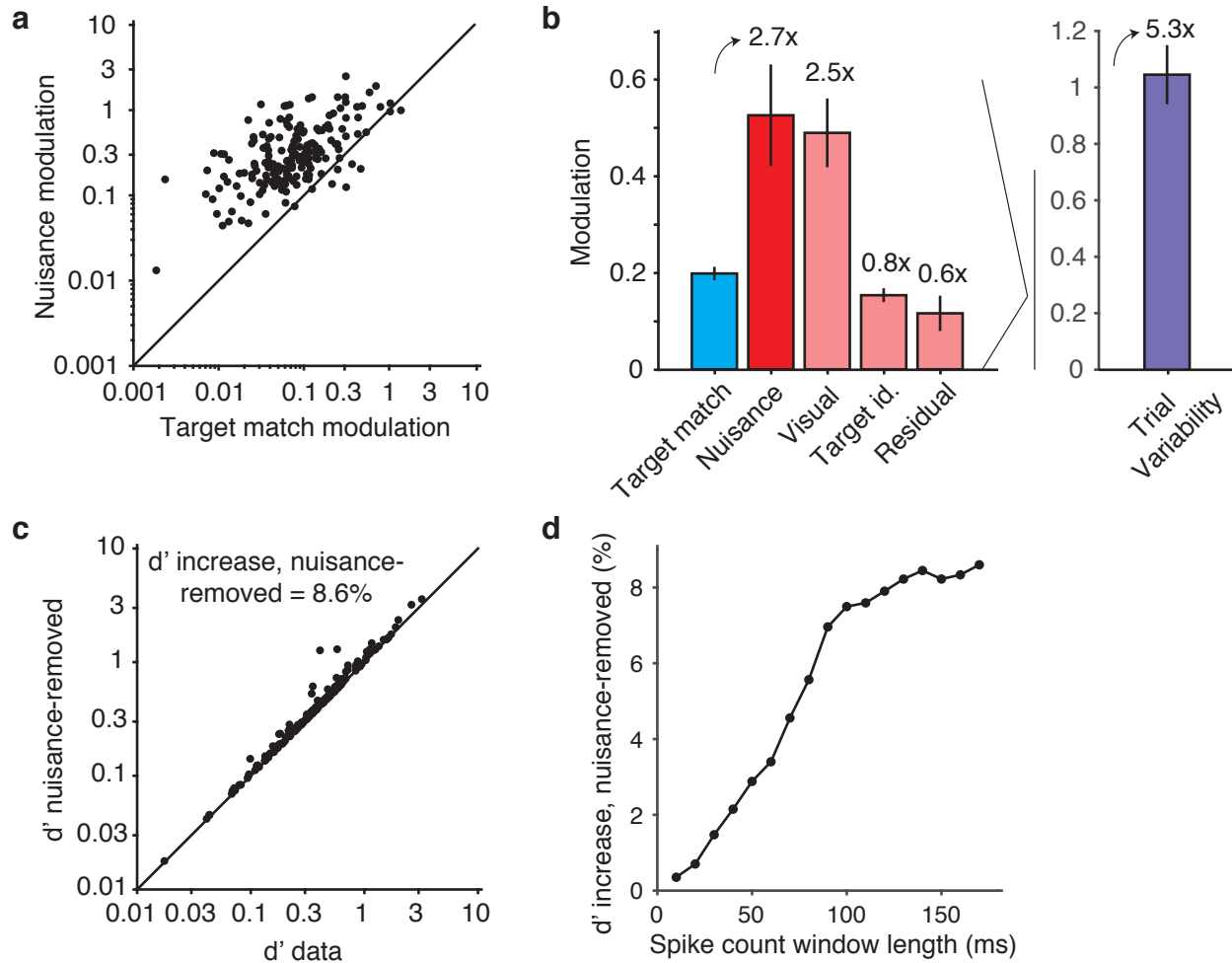




**Figure 4.** *The impact of nuisance modulation on single-unit  $d'$ .* Modulations were computed for each type of experimental parameter, in units of the standard deviations around each unit's grand mean spike count (see Results). **a)** Total nuisance modulation plotted against target match modulation for each unit. **b)** Average modulation magnitudes across units, parsed into target match modulation (cyan), combined nuisance modulation (dark red), and different nuisance modulation subtypes (light red) including visual, target, and residual. The right subpanel indicates the size of trial variability, computed with the same units. Error bars represent standard error across units. Numbers above each type of nuisance modulation indicate its size relative to the target match signal. **c)** Single-unit  $d'$  computed on the intact data and with the nuisance-term set to zero. The average proportional impact of nuisance was computed as the average proportional increase in performance when nuisance was removed. **d)** The impact of nuisance modulation on single-unit  $d'$  (computed as described in panel c), applied to spike count windows of increasing size.

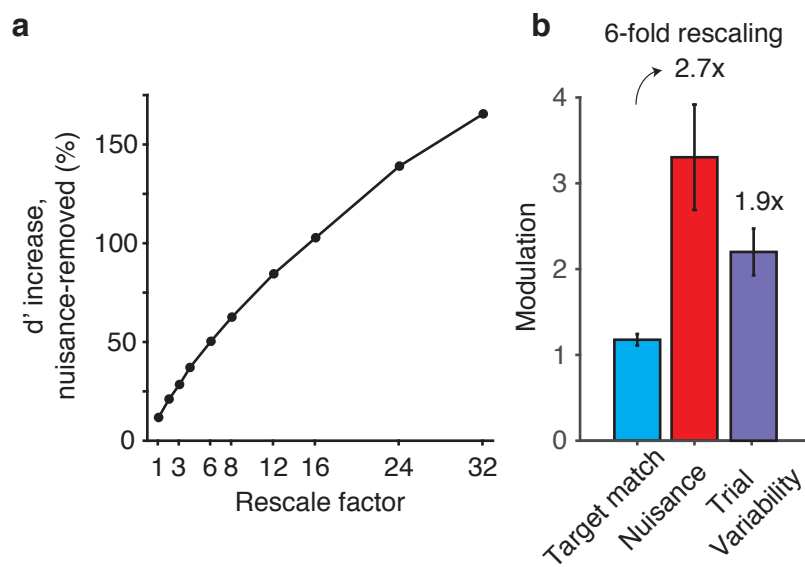


**Figure 5.** *Nuisance modulation is predicted to be detrimental for higher spike counts.* **a)** The simulated impact of nuisance modulation on single-unit  $d'$  as a function of rescaling the spike counts for each unit. **b)** Average modulation magnitudes across simulated units, for the 6-fold spike count rescaling data point in subpanel a.

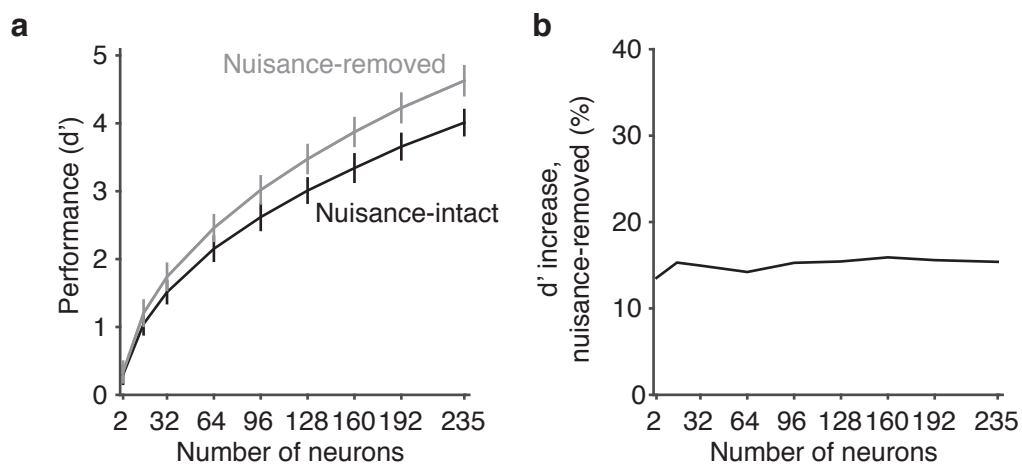
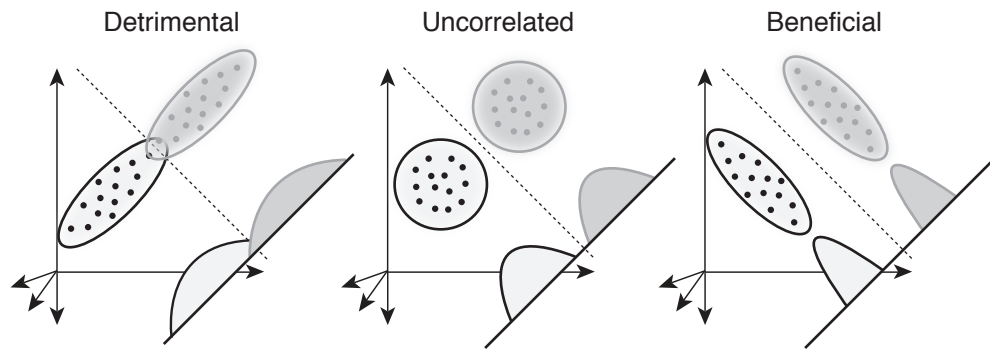


**Figure 6.** *Estimating the impact of nuisance modulation on population performance.* **a)** Linear decoder performance, shown in units of population  $d'$ , as a function of population size for two simulated populations: “Nuisance-Intact”: a version of our data in which the responses of each unit are replicated (after noise-correction), coupled with independent, Poisson trial variability; “Nuisance-removed”: a similar version of our data, but with the nuisance modulations for each unit removed. Error bars (SEM) reflect the variability that can be attributed to the random selection of units (for populations smaller than the full dataset) and the random assignment of training and testing trials in cross-validation. **b)** The proportional impact of nuisance (computed as the proportional increase in performance when nuisance was removed), plotted as a function of population size, computed for the data shown in panel a.

**a** Trial variability



**b** Nuisance modulation

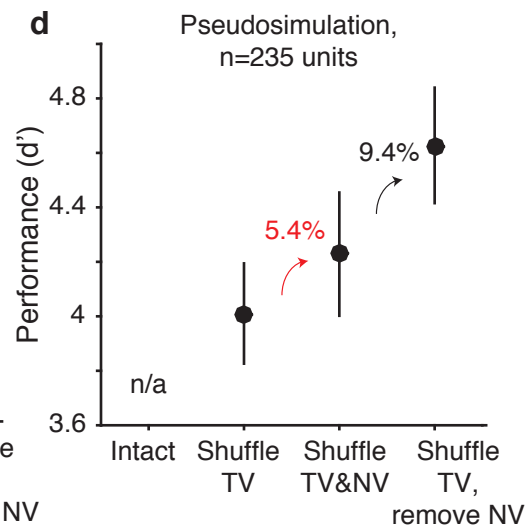
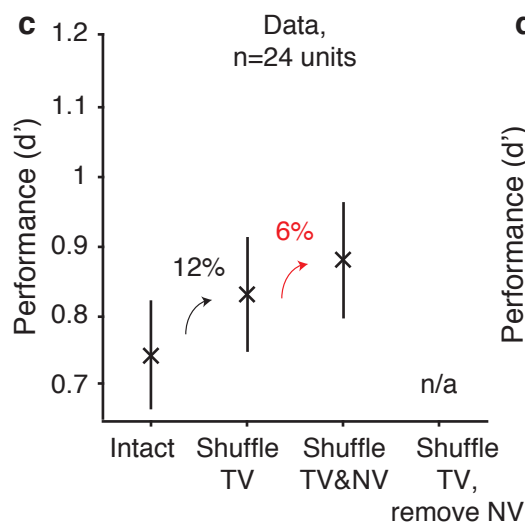
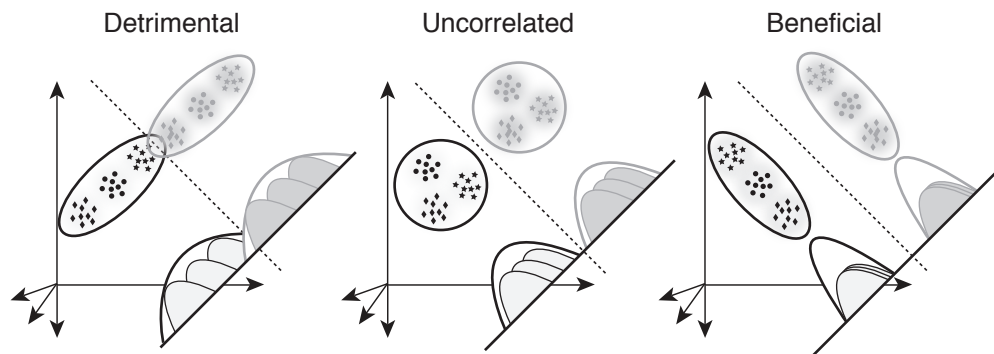




**Figure 7.** *Understanding how correlated trial variability and correlated nuisance modulations impact task performance.* **a)** Shown are cartoon depictions of the “beneficial” and “detrimental” impact that correlated trial variability can have on task performance relative to the “uncorrelated” benchmark. Each point depicts a hypothetical population response for a population of two neurons on a single trial, and clusters of points depict the dispersion of responses across repeated trials. Dotted lines depict the linear decision boundary optimized for a two-way classification. Population performance is determined by projecting each class onto an axis perpendicular to the decision boundary. Correlated trial variability between units can be configured to increase or decrease the variance of the projected population response relative to benchmark of uncorrelated trial variability, and thus have a detrimental or beneficial impact on performance. **b)** Same as in a, but expanded to incorporate correlated nuisance variability. Included are 3 experimental conditions within each set (clusters of points). Like trial variability, correlated nuisance variability between units can be configured to increase or decrease the variance of the projected population response, relative to benchmark of uncorrelated nuisance variability. **c)** To assess the impact that correlated trial and nuisance variability between units has on population performance, we applied shuffling procedures to the raw data recorded within each session. Shown is linearly decoded population performance ( $d'$ ) for populations of size 24 for: “Intact” – without shuffling; “Shuffle TV” – shuffled trial variability while maintaining nuisance variability correlations intact; and “Shuffle TV&NV” – shuffling both trial and nuisance variability. This analysis cannot be performed in a manner that assess what happens when nuisance variability is removed, thus the placeholder “n/a” for comparison with subpanel d. **d)** The same pseudosimulation data presented in Fig 6 ( $n = 235$ ). Because that data is simulated as independent between units, the “Intact” condition cannot be computed as indicated by n/a. Shown is “Shuffle TV”: linear decoding performance when trial variability is shuffled and nuisance variability is kept intact; “Shuffle TV&NV”: performance when trial variability and nuisance variability are shuffled; “Shuffle TV, remove NV”: performance when trial variability is shuffled and nuisance variability is removed. In both c and d, numbers above the arrows indicate the proportional increase in  $d'$ . Error bars (SEM) reflect the variability that can be attributed to the random assignment of training and testing trials in cross-validation.